FEBS Letters

FEBS PRESS science publishing by scientists

REVIEW ARTICLE

Labeling of virus components for advanced, quantitative imaging analyses

Volkan Sakin[1], Giulia Paci[2], Edward A. Lemke[2] and Barbara Müller[1]

1 Department of Infectious Diseases, Virology, University Hospital Heidelberg, Germany
2 Structural and Computational Biology Unit, Cell Biology and Biophysics Unit, European Molecular Biology Laboratory, Heidelberg, Germany

Correspondence
B. Müller, Department of Infectious Diseases, Virology, Universitätsklinikum Heidelberg, Im Neuenheimer Feld 324, 69120 Heidelberg, Germany
Fax: +49 6221 565003
Tel: +49 6221 561325
E-mail: Barbara_mueller@med.uni-heidelberg.de

(Received 3 February 2016, revised 8 March 2016, accepted 9 March 2016, available online 24 May 2016)

doi:10.1002/1873-3468.12131

Edited by Wilhelm Just

In recent years, investigation of virus–cell interactions has moved from ensemble measurements to imaging analyses at the single-particle level. Advanced fluorescence microscopy techniques provide single-molecule sensitivity and subdiffraction spatial resolution, allowing observation of subviral details and individual replication events to obtain detailed quantitative information. To exploit the full potential of these techniques, virologists need to employ novel labeling strategies, taking into account specific constraints imposed by viruses, as well as unique requirements of microscopic methods. Here, we compare strengths and limitations of various labeling methods, exemplify virological questions that were successfully addressed, and discuss challenges and future potential of novel approaches in virus imaging.

Keywords: amber suppression; click labeling; fluorescence; human immunodeficiency virus; imaging; nanoscopy; single-molecule techniques; virus

Viruses are obligatory intracellular parasites that enter a suitable host cell and usurp its functions to promote their own replication. Accordingly, viral life cycles comprise a series of intricate interactions of the virus with proteins, structures, and machineries of the host cell. The characterization of these interactions—not only qualitatively but also with respect to quantitative aspects—is paramount for a true understanding of virus replication.

Quantitative analysis of individual events in virus replication is a challenging task. *In vitro* studies using purified proteins only partially reflect the complex environment within a densely packed virion, a virus producing cell, or an infected organism. Ensemble measurements in tissue culture are hampered by the facts that (a) a large number of viruses interacts with a single cell in an asynchronous manner, (b) that different pathways may be followed in different cells in the cultured sample or even within the same cell, and (c) that interactions of viruses or viral proteins with host cell components are rapid and transient. Bulk measurements are therefore not well suited for capturing viral dynamics or for extracting quantitative information on individual replication steps.

In recent years, virological research has expanded from ensemble measurements to studies on single-cell and single-particle level, opening the door for quanti-

Abbreviations
FCS, fluorescence correlation spectroscopy; FPs, autofluorescent proteins; FRET, Foerster's resonance energy transfer; FRAP, fluorescence recovery after photobleaching; HBV, hepatitis B virus; HIV-1, human immunodeficiency virus-1; ICS, image correlation spectroscopy; ncAA, non-canonical amino acid; NLS, nuclear localization signal; NPCs, nuclear pore complexes; NTRs, nuclear transport receptors; ORF, open reading frame; PALM, photoactivated localization microscopy; PIC, pre-integration complex; POI, proteins of interest; RS, tRNAsynthetase; RTC, reverse transcription complex; SDCM, spinning disk confocal microscopy; SMLM, single-molecule localization microscopy; smFRET, single molecule FRET; STED, stimulated emission depletion microscopy; STORM, stochastic optical reconstruction microscopy; SVT, single virus tracking; TIRF-M, total internal reflection microscopy; vDNA, vRNA, viral DNA or RNA.

tative analyses of individual events or replication steps. This development is mainly owed to the availability of a broad range of genetically encoded autofluorescent proteins (FPs; [1,2]) for labeling viral proteins of interest (POI), together with groundbreaking advancements in fluorescence-based techniques. Single-molecule Foerster's resonance energy transfer (FRET), and fluorescence or image correlation spectroscopy (FCS or ICS) methods probe conformational changes or protein–protein interactions on a quantitative level [3–5]). Single-molecule localization microscopy (SMLM) and other super-resolution fluorescence microscopy techniques (here referred to as nanoscopy; [6,7]) reveal subviral structures and virus–host interactions in unprecedented detail [8]. Rapid time-resolved single virus tracking at the plasma membrane by total internal reflection microscopy (TIRF-M) or in 3D by spinning disk confocal microscopy (SDCM) allows quantitative analyses of entry events, dissects intracellular pathways, or elucidates dynamics of transient events [9–12]. Intravital microscopy follows the spread of the virus from one host cell to the next in a complex multicellular environment [13]. All of these methods require fluorescent labeling of one or more viral—and possibly cellular—component(s). Advancements in temporal and spatial resolution and single-molecule detection sensitivity, however, come at the cost of very specific requirements to the labels used. In addition, virus biology presents challenges for the introduction of genetically encoded labels. It could even be argued that labeling techniques have become a bottleneck that limits full exploitation of modern fluorescence-based techniques to obtain quantitative data on virological processes.

The primary prerequisite for interpretation of fluorescence data is a high molecular specificity of labeling. While this holds true for any fluorescence-based application, it becomes particularly relevant in the case of single-molecule techniques. Furthermore, single-molecule applications require particularly bright and photostable fluorophores. In addition, spectral properties of the fluorophore are an important consideration not only for multicolor or FRET-based applications but also in the context of investigating virus spread over prolonged time periods in tissue culture or by intravital imaging. Short wavelength illumination may adversely affect cell viability, and intravital imaging in deep tissues requires dyes in the infrared spectral range to minimize scattering.

Low cytotoxicity and cell permeability of the label are prerequisites for analyzing dynamic or transient events as well as for studying virus spread, and long-term observations at high frame rates rely on fluorophores with high photostability. Quantitative analyses in the cellular context have to take into account not only bleaching properties but also the pH- or redox-sensitivity of the fluorophore, which may alter fluorescence intensities according to the intracellular environment.

Nanoscopy allows unique insights into the architecture of virions and subviral complexes as the sub-diffraction resolution that can currently be achieved (~ 10–20 nm) is well below the size of many viruses. A requirement common to all nanoscopic principles (e.g., stimulated emission depletion microscopy, STED [14]; photoactivated localization microscopy, PALM [15,16]; or stochastic optical reconstruction microscopy, STORM [17]) is the ability of the chosen fluorophore to transition between a fluorescent state and a dark state: the quality of results depends on a high contrast between the 'on' and 'off' state of the label.

Finally, as nanoscopy advances to the molecular scale, the size and the localization of the fluorophore with respect to the POI also becomes relevant. While a ~ 20 nm distance between fluorophore and target protein resulting from indirect immunostaining may be negligible at the spatial resolution of conventional fluorescence microscopy, it significantly compromises the effective resolution in the case of nanoscopy. Intramolecular smFRET approaches for probing of protein dynamics and conformation also require precise localization of fluorescent probes at distinct positions within the molecule.

The most commonly used fluorescent labeling approaches—immunostaining and genetic labeling by fusion to an FP coding region—fall short in fulfilling many of these specific requirements. Immunostaining is typically not suited for live cell applications, prevents the precise positioning of the label, and may alter the dynamic properties of the target protein. It will therefore not be considered further in the scope of this review, whereas the use of FP fusions will be discussed in the following paragraph.

Imaging of viruses using autofluorescent proteins

The availability of genetically encoded FPs permits direct visualization of individual virus particles in live cells when they are fused to a virion-associated POI. Moreover, simultaneous labeling of different POI (e.g., surface and core components of a virion) in different colors provides new possibilities to study the biology of viruses. Employment of FP fusions in conjunction with time-resolved confocal or TIRF microscopy, FRET, fluorescence recovery after photobleaching (FRAP), or image correlation techniques can yield a wealth of information on the dynamics of cell uptake, intracellular trafficking, or particle assembly of a wide range of virus families.

Taking retroviruses as an example, one may outline a few key developments (for a more detailed review on results obtained using FP-labeled HIV-1, refer to 18,19). Incorporation of exogenously expressed FP-tagged HIV-1 viral protein R (Vpr; [20]) or integrase (IN; [21]) allowed the detection of individual virus particles and yielded seminal insights into the intracellular trafficking and nuclear import of HIV-1 subviral complexes entering a newly infected cell. The main HIV-1 structural polyprotein Gag has been successfully tagged with FP, either expressed alone [22,23], or in the context of partly functional HIV-1 derivatives [24,25]. These derivatives were used for quantitative characterization of Gag oligomer formation (e.g., [26,27]), dynamics of virus particle assembly [28,29], recruitment of viral RNA and cellular release factors to budding sites [30–32], as well as of HIV-1 cell attachment and uptake in different cell types (e.g., [33–35]). FP-tagged proteins from bacteriophages, which tightly bind to small cognate RNA hairpin motifs, were employed to label and track HIV-1 RNA within live cells (e.g., [31,36–38]). FP-tagged HIV-1 nucleocapsid (NC) protein or free FP released by the activity of the viral PR within the particle were used as viral soluble content markers to define the time point of membrane fusion for analyses of the HIV-1 entry process (e.g., [39,40]). Nanoscopic images of the architecture of HIV-1 assembly sites were obtained with the help of Gag derivatives carrying the photoconvertible FP mEos (e.g., [41–43]). Retroviruses tagged with FP at either Gag or envelope glycoprotein (Env) revealed 'surfing' of retroviruses along filopodia from infected to uninfected target cells [44]. Moreover, they helped to visualize the formation of virological synapses between infected cells and new host cells and the cell-to-cell transmission of viral structural proteins in tissue culture (e.g., [24,45,46]). Finally, recent studies using FP-labeled virus provided exciting insights into the capture and subsequent dissemination of retroviruses by macrophages in lymphoid tissues of living mice [47].

The application of FPs has yielded numerous important insights by opening a window for direct observation of viruses within live cells and tissues. However, the approach is limited with respect to many advanced fluorescence-based applications. Moreover, the size of the FP insertion also presents an obstacle for the tagging of viral proteins, as outlined below. Consequently, a derivative of HIV-1 carrying FP within the virus particle that permits robust replication over multiple rounds and spread in different target cell types has not been described to date.

Beyond autofluorescent proteins: labeling strategies using synthetic fluorophores

Advantages of synthetic fluorophores

Starting with the discovery and biological application of the GFP, a continuously increasing panel of FPs has been developed, which not only spans a broad range of colors but also includes photoswitchable and photoconvertible variants as well as fluorescent sensor molecules [1,2,48]. However, the infrared range of the spectrum, particularly relevant for intravital imaging in deep tissue, is currently not well covered by FPs. Most importantly, although photophysical properties vary between different FPs, photostability of modern fluorescent dyes is generally orders of magnitude higher than that of FPs [7], rendering synthetic fluorophores superior for single-molecule techniques (e.g., STORM, smFRET), applications requiring high laser power (e.g., STED), or long-term live cell observations with high frame rates. A major advantage of synthetic dyes for observing dynamic events in virus replication is that fluorescence is an inherent property of the molecule, whereas FPs need to undergo oxygen-dependent chemical maturation as rate-limiting step in fluorophore synthesis [49]. Maturation times in the range of several minutes to hours, depending on the protein and environmental conditions, render FPs invisible during the initial time window following translation (e.g., during trafficking of a viral structural protein to the assembly site), and incomplete maturation of fluorophores can impair quantitative readouts. In addition, misfolding and/or post-translational modification of FPs in oxidizing cellular environments, such as the secretory pathway or the inner membrane space of mitochondria, can result in a pool of FP molecules in a dark state [50].

Moreover, a given FP-tagged protein variant has specific photophysical properties; altering these properties (e.g., changing the color of the fluorophore to adapt for a different experimental setting) requires construction and characterization of a new tagged variant. Although FPs share a similar beta-barrel structure, they differ in folding kinetics, oligomerization propensity, and exposed surface residues; thus, exchanging an FP moiety to a variant with a different color can alter the functionality of the fusion protein. Staining with synthetic dyes, in contrast, offers more flexibility and allows researchers to explore novel fluorophores provided by chemical biology.

A major advantage of chemical dyes over FPs in the viral context is their small size and flexible positioning within the POI, as outlined in the following section.

A difficult target: virus-specific challenges for FP labeling strategies

A FP moiety with a molecular weight of 27 kDa may significantly affect functionality and intracellular localization of any POI, in particular when targeting internal sites within the polypeptide. Beyond this general concern, viruses present unique difficulties for the insertion of genetically encoded labels. To allow for packaging into the defined volume of the virus capsid, viral genomes are generally characterized by a limited coding capacity. Therefore, viruses often employ small, multifunctional proteins that are involved in various protein–protein, protein–nucleic acid, or protein–lipid interactions. Fusion to an FP moiety with a hydrodynamic radius of 2–3 nm—equal to or exceeding that of the viral target protein (Fig. 1)—may easily affect protein functionality. This concern is particularly relevant for viral capsid proteins, which multimerize into highly ordered structures sensitive to disruption by the addition of extra protein domains. In the crowded context of assembling capsid structures not only obligatory multimeric FPs but also monomeric FP variants with a residual tendency to oligomerize at high local concentrations [51] may be detrimental. Furthermore, overlapping ORFs, employed by many viruses as a strategy of genetic economy, can result in the unwanted change of overlapping ORFs upon tag insertion. Finally, inserting ~ 750 base pairs of FP coding sequence increases genome size substantially for many viruses (e.g., ~ 8% in the case of HIV, or ~ 23% in the case of hepatitis B virus, HBV) and may thereby affect genome packaging or genetic stability. Particular replication strategies employed by viruses are prone to genetic recombination events, compromising the stability of foreign insertions over multiple rounds of replication.

Traditional chemical protein labeling methods make use of naturally occurring reactive groups in the POI which present targets for covalent coupling to functionalized dye molecules. Targeting primary amines present at N-termini or at surface exposed lysine residues by *N*-hydroxysuccinimidyl esters, as well as chemical coupling of dyes to sulfhydryl groups of reduced cysteines via the maleimide-thiol reaction are well-established techniques that have also been successfully applied in virology. However, their application is limited by the facts that they rely on the presence of reactive residues at the site of interest and that labeling density may not be easy to control. Importantly, molecular labeling specificity is achieved by performing the coupling reaction on highly purified material *in vitro*, which essentially restricts these approaches to the labeling of (mostly nonenveloped) gradient purified virus particles for studying cell attachment, receptor binding, or virus uptake [10].

These limitations are addressed by strategies that combine site-specific introduction of genetically encoded tags harboring unique functionalities with their specific coupling to synthetic dyes. The following sections, Figs 1 and 2 and Table 1, briefly outline different alternative principles.

Self-labeling enzyme derivatives

The development of self-labeling enzyme derivatives greatly expanded the flexibility and versatility of genetic labeling approaches. There are numerous variations of this theme, with the SNAP-tag [52], CLIP-tag [53], and HaloTag [54] representing widely known examples (Fig. 1). These proteins are derivatives of O6-alkylguanine transferase (SNAP- and CLIP-tag) or haloalkane dehalogenase (HaloTag), genetically engineered to accept fluorophore-linked substrate analogs as suicide inhibitors for covalent attachment of the fluorophore to the enzyme's active site [52–54]. Substrate analogs attached to a variety of synthetic fluorophores (as well as other functional groups, e.g., biotin) are available and continue to be developed, offering flexibility to use a single genetically tagged derivative in different experimental settings [5]. Although SNAP- and CLIP-tag are based on the same enzyme, distinct substrate specificities permit their use for dual-labeling strategies [53]. The TMP-tag is based on the high-affinity noncovalent interaction between *Escherichia coli* dihydrofolate reductase and trimethoprim; engineered versions of the tag allow for covalent attachment of fluorescent trimethoprim derivatives [55].

Stainable peptide tags

While the stainable protein tags described above are more versatile than FPs, they are not significantly smaller in size (Fig. 1). Stainable peptide tags present an alternative option when the size of the inserted coding sequence and/or the attached protein moiety is a relevant issue. A prominent example is the tetracysteine tag (TC-tag or FlAsH-tag) described by Tsien and coworkers [56]. A 6–12 amino acid long peptide sequence comprising four cysteine residues introduced into the POI forms high-affinity noncovalent complexes with biarsenical dyes (FlAsH or ReAsH; [56]),

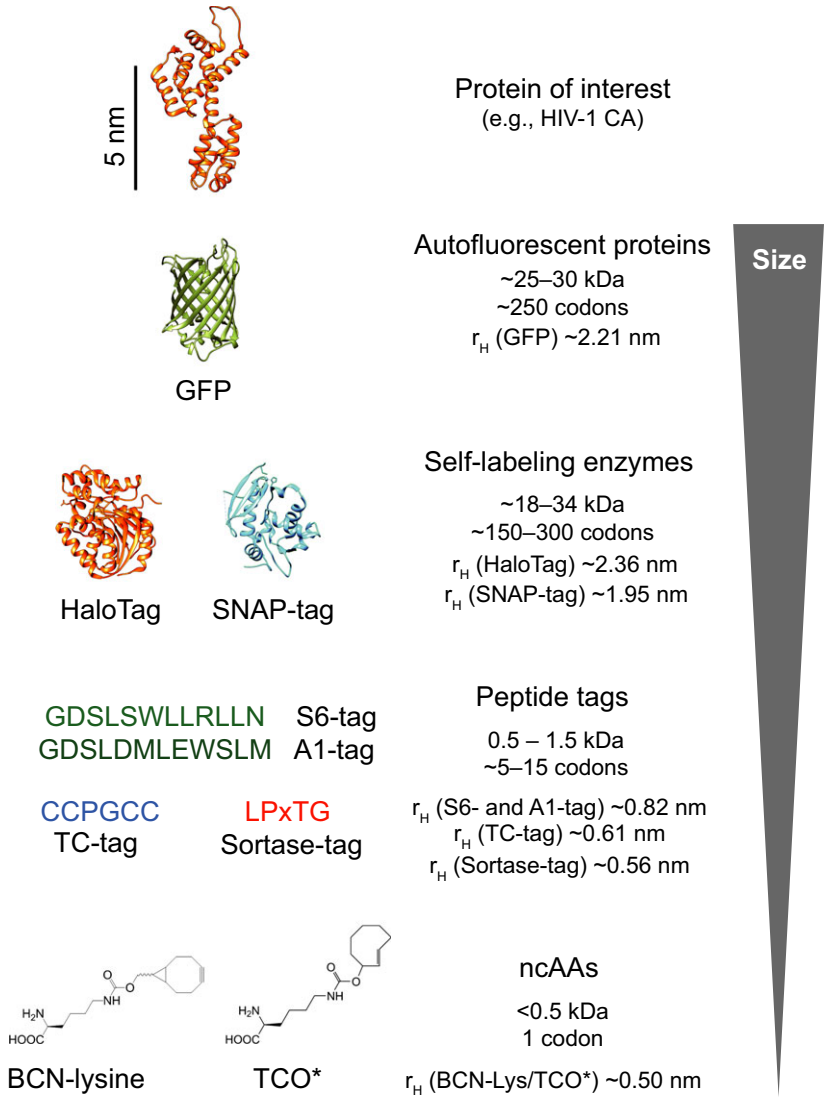

Fig. 1. Genetically encoded labels vary in mass and size. The scheme shows examples of an autofluorescent protein, self-staining protein tags, peptide sequences of exemplary stainable peptide tags, and ncAAs. Protein tags are represented to scale in comparison to an exemplary viral POI (HIV-1 CA). PDB accession codes used for the protein structures 1EMB (GFP), 3KZY (SNAP-tag), 4KAA (HaloTag), and 4XFX (HIV-1 CA). Hydrodynamic radii r_H were estimated based on molecular masses according to the formula, $r_H = 0.75$ Mr 0.33 A, with the assumption that proteins are in their native state [138].

resulting in a strong enhancement of dye fluorescence. Its self-labeling capacity, together with the small size, makes the TC-tag a very attractive tool. Limitations are the small selection of cognate dyes, the presence of four reactive cysteines with oxidation-sensitive sulfhydryl groups within the tag, and a high propensity for intracellular background staining.

Other peptide tags which have been developed represent target sequences for specific enzymes that mediate covalent attachment of functionalized fluorescent molecules to the peptide sequence. Peptide substrates recognized by the bacterial enzymes sortase A (Sortase-tag; [57]), transglutaminase (Q-tag, [58]), phosphopantetheinyl transferases (PPTases) such as acyl carrier protein synthase (AcpS) and Sfp (A1- and S6-tag, respectively) [59,60], and lipoic acid ligase (LAP-tag; [61]) belong to this class. While the Sortase-tag imposes restrictions with respect to the placement of the tag within the POI, and most of the labeling enzymes need to be added as purified proteins in an *in vitro* labeling reaction (thereby limiting targets to surface expressed proteins), lipoic acid ligase can be exogeneously expressed in eukaryotic cells. Labeling of intracellularly expressed POIs carrying the cognate

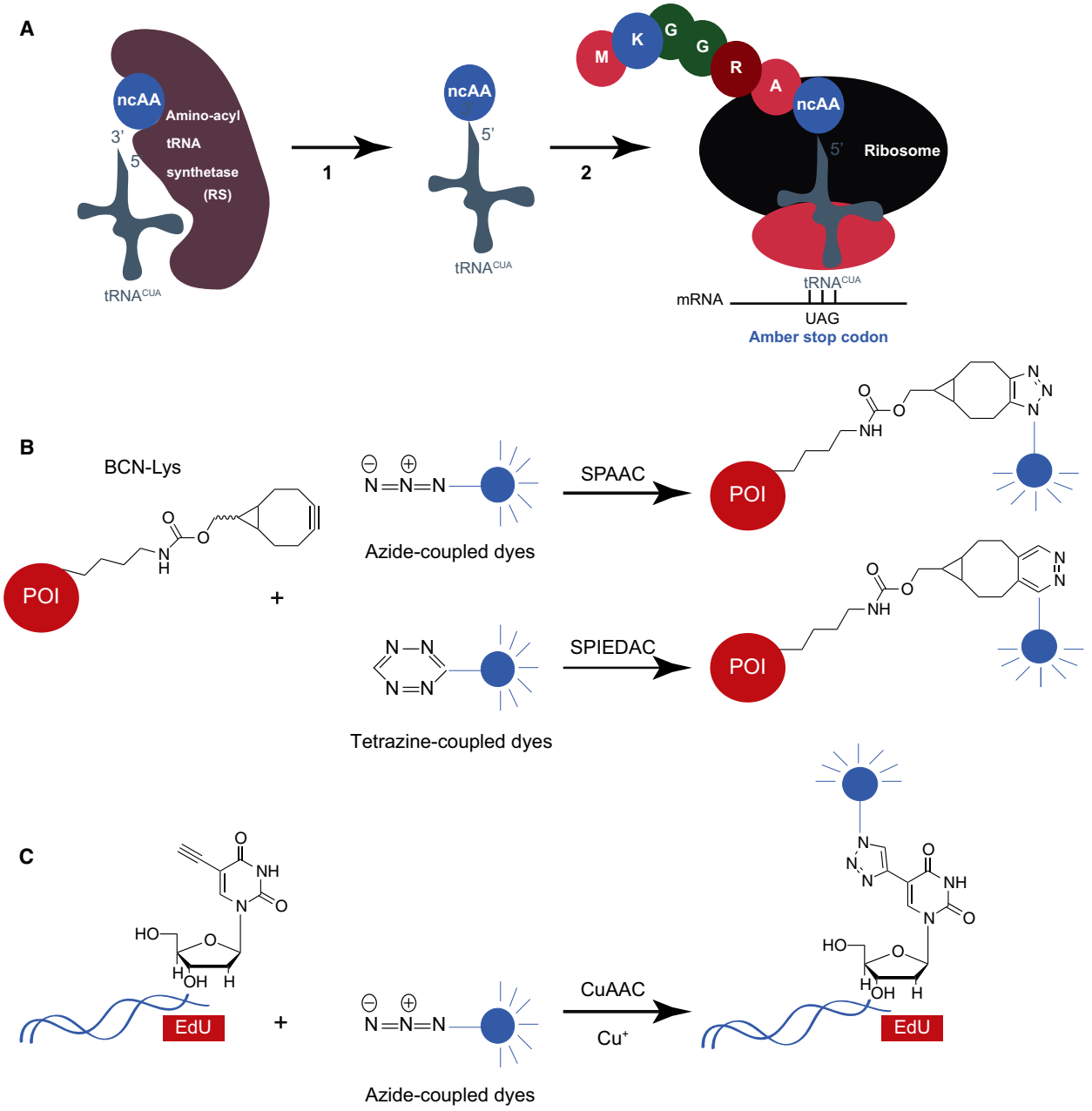

Fig. 2. Schematic representation of minimally invasive labeling strategies. (A) Incorporation of ncAA by amber suppression. A viral genome, or an expression vector, encoding the POI carrying a TAG at the target position is transfected into a suitable cell line together with one or two expression vector(s) encoding the orthogonal RS/tRNA^{CUA}. In the first step, the engineered RS charges the 3′ end of tRNA^{CUA} with the ncAA. Subsequently, the charged tRNA^{CUA} recognizes an UAG codon in the mRNA bound to the ribosome and adds the ncAA to the growing polypeptide chain. (B) Cu(I)-independent click labeling of proteins. An ncAA with a strained alkyne group (e.g., BCN-Lysine, as shown here) incorporated into the POI by amber suppression (A) can undergo two Cu(I)-independent bio-orthogonal reactions: strain-promoted alkyne–azide cycloaddition (SPAAC) with azide-coupled fluorophores, or strain-promoted inverse electron-demand Diels–Alder cycloaddition (SPIEDAC) in the presence tetrazine-coupled dyes (C) Labeling of nucleic acids by Cu(I)-catalyzed azide–alkyne cycloaddition (CuAAC). A viral polymerase incorporates a nucleoside analog with a linear alkyne moiety, e.g., EdU (5-ethynyl-2′-deoxyuridine) as shown here or EU (5-ethynyl uridine), into newly synthesized viral DNA (or RNA) in cells. Upon addition of azide-coupled fluorescent dyes, the modified nucleic acid can be specifically labeled in fixed cells.

Table 1. Advantages and limitations of protein labeling strategies.

Method	Advantages	Limitations	References for use in virology
Fluorescent proteins	No need for staining; live-cell compatible; inherent specificity of labeling	Large size; restricted photophysical properties and spectrum range; oligomerization; maturation time of fluorophores	[18,19]
Self-labeling enzymes	Broad range of available dyes; flexible; superior photophysical properties; live-cell compatible	Large size; limited choice of cell-permeable dyes	[123]
Stainable peptide tags	Small; site specific; flexible		
TC-tag	Self-labeling; live-cell compatible	Only two cognate dyes available; background staining; oxidation sensitive	[86,93,125]
E.g. A1-, S6-, Sortase-,LAP-tag	High specificity of labeling; broad range of available dyes	Need for recombinant cognate enzyme; mostly limited to cell surface or *in vitro* labeling	[88,128]
Click chemistry	Minimally invasive; site specific; flexible		
CuAAC	Efficient labeling; well established for *in vitro* studies and fixed samples	Cu(I) dependent; limited to fixed samples	[80,81,94]
SPAAC and SPIEDAC	Live-cell compatible; broad range of ncAAs with different chemical properties	Requires orthogonal tRNA/RS; limited choice of cell-permeable dyes	[76,77]

LAP-tag peptide has been demonstrated [62], broadening the spectrum of potential applications.

Site-specific protein labeling using bio-orthogonal chemistry

Even the insertion of a few amino acids may be deleterious for a given POI, especially in a viral context. A powerful solution to this problem is exploiting the promiscuity of native aminoacyl tRNA synthetases (RS) to accept alternative substrates for aminoacylation of their cognate tRNA (e.g., replacement of methionine with seleno-methionine by growing *E. coli* in appropriate minimal media [63]). This method has been extended to encode a variety of noncanonical amino acids (ncAAs) [64], which in turn opens possibilities to introduce designed functional groups or fluorescent dyes by bio-orthogonal chemistry.

For site-specific labeling of a specific POI via an ncAA, a stop codon is introduced into the POI coding sequence at the site of interest and the host organism is engineered with an orthogonal tRNA/RS pair, i.e., not cross-reactive with any of the endogenous tRNA/RS pairs ([65], Fig. 2A). The substrate specificity of the RS is altered to strongly prefer a custom designed ncAA to its native substrate and the tRNA is typically tuned to recognize the TAG amber stop codon. The method is thus frequently referred to as amber suppression, albeit other codons have also been reprogrammed [66]. The technique has proven to be transferable to a variety of eukaryotes, *from S. cerevisae* to different mammalian cells [66] as well as multicellular organisms like *C. elegans* and *Drosophila melanogaster* [67,68].

Although the tolerance of the host cell translational machinery against modifications is not endless, about 200 ncAA have been genetically encoded to date [66,69]. A focus has long been to genetically encode biocompatible functionalities, such as clickable groups (i.e., nontoxic groups that react in water specifically and fast [70]) suitable for subsequent labeling with a fluorophore [71,72]. Among those, ring-strained alkynes and alkenes have recently gained much attention, as they permit strain-promoted azide–alkyne cycloadditions (SPAACs) and strain-promoted inverse electron-demand Diels–Alder (4 + 2) cycloaddition (SPIEDAC), respectively [73–75] (Fig. 2B). SPAAC- and SPIEDAC-functionalized ncAAs can react with a variety of azide or tetrazine derivatives of many commercially available fluorophores. An increasing number of live cell applications are described [70], including proof-of-principle reports on the staining of viral surface proteins on isolated virus particles [76] or on the host cell membrane [77].

Labeling other viral components

Bio-orthogonal click chemistry not only opens novel possibilities for protein labeling but also offers approaches for labeling of other components of the

virion. The key component of any virus is its genome, consisting of DNA or RNA depending on the virus family. It is the only viral feature consistently present in the 'eclipse' phase between cytoplasmic entry and production of virus progeny that is the hallmark of all viral replication cycles.

Incorporation of bio-orthogonal nucleotide derivatives [e.g., 5′ethynyl uridine (EU) or 5′ethynyl-2′deoxyuridine (EdU)] into newly synthesized nucleic acid introduces functional groups that can subsequently be targeted for specific coupling to functionalized dye molecules in a copper-catalyzed click reaction [78,79], (Fig. 2C). Albeit this approach is inherently nonspecific, i.e., all newly synthesized DNA or RNA within the cell will be labeled; specificity may be introduced by the viral system. Large amounts of viral genomes are synthesized during the productive phase of the replication cycle; in many cases, genome replication occurs at distinct virus-specific sites (e.g., RNA viruses replicating in large 'factories' in the cytoplasmic region; retroviruses performing DNA synthesis within subviral complexes in the cytosol). Furthermore, virus particles carrying functionalized genomes can be purified and used to infect host cells whose own nucleic acids are unmodified (e.g., [80,81]).

The viral lipid envelope and gylcoproteins on the outer viral surface present additional potential targets for bio-orthogonal labeling. Azido-sugars added to the culture medium are metabolized and incorporated into cell-surface glycans, which are subsequently conjugated to a cyclooctyne-conjugated imaging probe [82]. Again, this approach does not specifically target viral glycoproteins, but selectivity is achieved by labeling using purified virus samples. Employing this strategy, adenovirus particles could be labeled upon incorporation of *O*-linked *N*-azidoacetylglucosamine into the viral fiber protein [83]. Furthermore, clickable lipid orthologs have been synthesized [84], which can be expected to develop into useful tools for future virological studies.

Viruses in the spotlight: glimpsing into viral replication cycles

While still under development and largely employed in proof-of-principle studies, the novel labeling approaches discussed in the previous sections start to yield some important insights into virus biology, demonstrating their future potential.

Although viral replication strategies vary widely between different families, all viral replication cycles comprise common generic steps, which are outlined in Fig. 3 (a-h). Host cell attachment (a) and uptake (b) are followed by uncoating of the capsid structure releasing the viral genome (c). Genome replication (e) and synthesis of virion components (f) are performed with the help of the host cell. Finally, progeny viruses are assembled (g) and released (h) from the virus-producing cell. Whereas some virus families replicate exclusively within the cytoplasm, transport of viruses or subviral complexes to the nuclear pore and import of the viral genome into the nucleus (d) are essential steps in the replication cycle of many other viruses (including HIV-1).

Novel labeling and imaging approaches have been recently employed to gain detailed and quantitative insight into individual parts of viral replication cycles, as illustrated by some examples summarized in Fig. 3 (i-ix). For the following discussion, we will focus mainly on retroviruses, in particular HIV-1, including only some examples from other virus families. We apologize to all colleagues, whose important work could not be cited for the sake of brevity.

Virus cell entry

Viral replication cycles are initiated by attachment to suitable host cells and entry into the cytoplasm mediated by specific molecules on the virus surface. For enveloped viruses, viral glycoproteins inserted into the lipid envelope mediate fusion of the virus with a lipid membrane of the host cell. Tagging of viral envelope proteins with FPs without interfering with membrane trafficking and glycosylation, particle incorporation, receptor binding, and fusogenic activity is challenging, highlighting the relevance of minimally invasive strategies.

The key molecule in the case of retroviruses is the Env transmembrane glycoprotein inserted into the lipid envelope of the particle. HIV-1 Env is a trimeric complex of gp120/gp41 heterodimers, which mediates virus entry via sequential interactions with the CD4 receptor and coreceptors on the host cell membrane. Interaction of gp120 with CD4 leads to a conformational rearrangement of the Env protein, exposing a second binding surface on gp120 that interacts with a coreceptor molecule (CCR5 or CXCR4). This in turn results in conformational rearrangements within gp41 that promote fusion of the viral envelope with the host cell membrane [85]. Although HIV-1 Env structure and its function in the viral entry process have been intensely studied over the last three decades [85], structural models of Env represent static views of distinct stages, while the crucial dynamics of conformational rearrangements could not be addressed.

Live cell imaging studies using labeled HIV-1 Env protein are hampered by the facts that its functionality

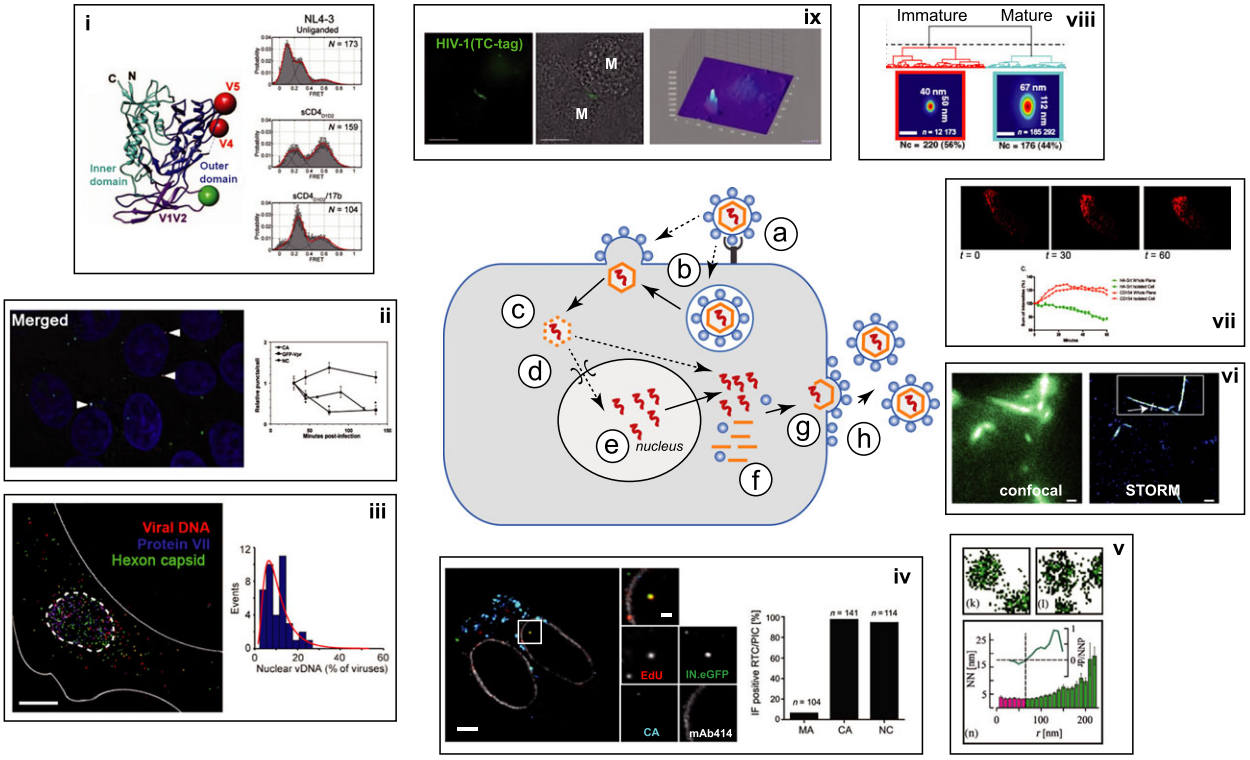

Fig. 3. Generic viral replication cycle (a–h) and examples for results obtained on individual replication steps using site-specific chemical labeling approaches (i–ix). Infection starts with virus attachment and binding to cellular receptor(s) (a). Dependent on the virus, uptake and cytoplasmic entry of the viral capsid (b) can occur through various different pathways. Capsid uncoating (c) releases the viral genome; in the case of some viruses, nuclear import of the genome (d) is an obligatory step. Genome replication (e) and synthesis of viral proteins are achieved through use of cellular machineries (f) and are followed by virus particle assembly (g) and release (h). Again, intracellular localization of assembly sites and release pathways vary between different virus types. (i–ix) Chemical labeling strategies can be employed to investigate individual aspects of viral replication. (i) smFRET analyses of HIV-1 Env molecules labeled by site-specific insertion of A1/Q3 peptide tags revealed an equilibrium between distinct conformational states [88]. (ii) Step-wise dissociation of virion proteins from entering HIV-1 RNA complexes was visualized by EU/click labeling of viral RNA [81]. (iii) Following individual virus genomes by EdU/click labeling revealed nuclear import of the genome as a bottleneck for adenovirus entry [80,139]. (iv) Visualization of nascent viral cDNA in HIV-1-infected cells by EdU/click labeling showed association of RTCs with viral proteins and detected nuclear import of PICs [94]. (v, vi) High-resolution imaging of virus assembly sites at the plasma membrane of host cells employing HIV-1-carrying SNAP-tagged (v), or influenza virus-carrying ncAA/click-labeled (vi), structural proteins [77,124]. (vii) Sortase-tagging of influenza virus HA glycoprotein expressed in the viral context was employed to analyze dynamics of protein turnover at the plasma membrane [128]. (viii) Distinction between immature and mature HIV-1 particles in PALM images based on intravirion distribution patterns of TC-tagged IN [127]. (ix) Transmission of HIV-1 via virological synapses between infected and uninfected macrophages, visualized using viruses carrying a TC-tag within the main structural protein Gag [125]. Images in (i)–(ix) have been modified from the cited references, with permission.

is apparently compromised by larger insertions, and that only 10–15 Env trimers are incorporated per virion. The variable loops V4 and V5 of gp120 have been reported to tolerate insertion of a TC-tag [86] or an optimized version of GFP [87] while retaining partial to nearly full fusogenic activity. These concepts have, however, not been further explored. Given the low number of Env on the particle surface, brighter and more photostable fluorophores would be desirable for SVT analyses.

A breakthrough in the understanding of HIV-1 Env dynamics has recently been achieved by single-molecule analyses assessing the conformation of the protein *in situ* [88] (Fig. 3i). Employing insertion of A1 and Q3 peptide tags followed by enzyme-mediated staining with synthetic dyes (see above), the authors generated Env molecules carrying two labels at defined sites within the V1 and V4 loop of the molecule. Conformational states of single HIV-1 Env molecules on the surface of individual virions could then be captured in smFRET measurements, revealing a dynamic equilibrium between three distinct states whose relative population was quantitated under different conditions [88]. The binding of CD4 and coreceptor resulted in

significant stabilization of two 'open' conformational states not frequently populated in the unliganded molecule. However, broadly neutralizing antibodies stabilized the 'ground state' of the molecule, providing an explanation for their inhibitory action and suggesting that vaccines mimicking Env locked in the ground state may display increased potential to elicit a neutralizing antibody response [88].

Uncoating and intracellular trafficking

Once the viral genome has been delivered into the cytosol, it needs to be transported to the site of replication. Depending on the virus, this site may be either the nucleus or a distinct compartment in the cytoplasm, and transport may occur within intracellular vesicles and/or as free viruses or subviral complexes along cytoskeletal filaments. Many virus particles may be taken up into a single host cell in a nonsynchronized manner. They often follow multiple different (productive as well as abortive) pathways, which precludes analysis by ensemble measurements. Imaging individual virus particles to directly follow cell attachment and entry in quantitative SVT experiments made this part of the replication cycle amenable to study, allowing to dissect trafficking pathways and measure transport velocities [11,12,89]. Following cytoplasmic entry of the capsid, the viral genome is released by capsid uncoating. As uncoating and loss of other virion-associated proteins may occur before or during intracellular trafficking, functionalized nucleotide derivatives for labeling the viral genome as the only consistent *bona fide* component during the postentry phase are of particular interest in this context.

Wang and coworkers [80] (Fig. 3iii) exploited adenovirus metabolically labeled with ethynyl-modified nucleosides to analyze postentry events in newly infected cells. Upon uncoating of the viral capsid at the nuclear pore, incoming viral DNA genomes (vDNA) became accessible to click labeling by Cu(I)-catalyzed azide–alkyne cycloaddition, permitting detection at single-molecule resolution. The time course of postentry events was studied by quantitating vDNA molecules at different intracellular localization and different time points, in conjunction with immunostaining of the viral capsid protein and the vDNA-associated protein VII. Unexpectedly, a significant proportion of capsid-free vDNA was detected in the cytosol, indicating that nuclear import of the viral genome represented a bottleneck in the adenoviral replication cycle [80].

In the case of HIV-1, the conical capsid encasing the genomic RNA is released into the cytoplasm. Based on biochemical analysis of isolated subviral complexes from freshly infected cells, capsid uncoating was presumed to occur rapidly, followed by reverse transcription of the RNA genome and transport of the cDNA copy, associated with viral (and cellular) proteins to subviral nucleoprotein complexes (reverse transcription complex, RTC, and preintegration complex, PIC, respectively) of the nucleus [90]. However, several lines of evidence accumulated in recent years clearly argue against the immediate loss of capsid after virus entry. Work from many labs studying the early postentry events by mutational analyses of capsid or small molecule inhibitors affecting capsid stability demonstrated that uncoating, reverse transcription and nuclear import are temporally and functionally interwoven in a complex fashion that is extremely difficult to dissect through ensemble measurements [91,92]. Whether capsid uncoating is a gradual process or is only initiated at the nuclear pore remains a matter of debate.

Dynamics of cytoplasmic trafficking of subviral complexes was analyzed by SVT after labeling of core components of the RTC/PIC (IN tagged at its C-terminus by a TC-tag or Vpr fused to GFP), revealing that long-range cytoplasmic transport occurred in a microtubule- and dynein-dependent manner [20,93]. The viral capsid was not followed in these analyses.

A recent indirect approach utilized virions containing EU incorporated into the viral genome [81] (Fig. 3ii). The functionalized viral RNA (vRNA) was not accessible to click chemistry staining while packaged within a closed capsid shell. Time-lapse image analyses in freshly infected cells revealed initial appearance of a dense, NC-associated vRNA signal. This signal was subsequently lost, consistent with instability or diffusion of vRNA in the cytosol, and the kinetics of signal loss were affected by mutants or small molecule compounds known to affect capsid stability. Based on these observations, the authors suggested that HIV-1 uncoating occurs in two distinct steps: an initial opening of the closed capsid structure, followed by complete dissolution of the capsid shell [81].

A key problem of imaging studies investigating viral entry processes is that virus particles not only enter through a productive pathway but may also be taken up via nonspecific and unproductive routes. Depending on the virus and cell type, unspecific uptake may represent the vast majority of events observed in tissue culture. Assignment of individual productive events is therefore crucial for interpretation of imaging data. In the case of HIV-1, loss of virion-incorporated FP as a viral content marker can be used to differentiate between intact virus, virions that have undergone membrane fusion, and those that underwent subsequent

opening of the capsid [40]. More directly, productive RTCs can be identified by labeling of newly synthesized viral cDNA in the cytoplasmic region of infected cells. In a seminal study, cDNA visualization was accomplished by microinjection of fluorescently labeled dNTPs for incorporation into nascent viral DNA [20], but the approach was not feasible for quantitative analyses. Recently, incorporation of EdU followed by bio-orthogonal labeling in conjunction with GFP-labeled IN as a *bona fide* component of postentry complexes allowed robust detection of functional HIV-1 RTCs or PICs in infected cells and permitted quantitative assessment of RTC/PIC association with key viral and cellular proteins by immunostaining [94]. These experiments revealed association of CA with nearly all productive cytoplasmic HIV-1 RTC/PIC (regardless of their distance from the nuclear envelope) with a similar intensity to that of complete virions, indicating that a capsid-like structure may be retained throughout cytoplasmic transport.

More detailed investigation of HIV-1 uncoating dynamics awaits the development of a direct capsid-labeling strategy suitable for live cell experiments. As CA is highly sensitive to genetic alterations, with insertion of the small TC-tag in an exposed surface loop [95] or even single point mutations (e.g., [96,97]) severely compromising viral replication competence, establishment of a minimal invasive labeling strategy will likely be necessary.

Nuclear import

Transport of the viral genome into the postmitotic nucleus is an essential step in the life cycle of many viruses (e.g., HIV-1 and other lentiviruses, adenoviruses, herpesviruses, influenza viruses, HBV, baculoviruses). Physiological transport of macromolecules between cytoplasm and nucleus occurs through nuclear pore complexes (NPCs), large supramolecular structures with an estimated molecular mass of ~ 120 MDa in metazoa [98]). The striking transport capacity of a single NPC allows ~ 1.000 translocation events per second [99].

Nucleocytoplasmic transport allows passive diffusion of small molecules (< 40 kDa), whereas bigger cargoes cross the NPCs through facilitated diffusion by binding to nuclear transport receptors (NTRs). The majority of NTRs belong to the β-karyopherin family and recognize specific nuclear localization and export signals (NLSs and NESs, respectively) present on the cargoes, either directly or indirectly via adaptor proteins. Several strategies have been developed by viruses in order to hijack the nuclear transport machinery [100,101]: some small viruses apparently cross the NPC as intact particles (e.g., HBV or baculoviruses), others dock at the cytoplasmic side of the NPC and release their genetic material through an uncoating process (e.g., adenoviruses). Among the viruses that exploit the cell's nuclear transport machinery, some bear viral proteins with classical NLSs (e.g., SV40 large T-antigen), whereas others employ noncanonical NLSs (e.g., influenza virus nucleoprotein). In other cases (e.g., HIV-1), the karyophilic principle remains yet to be determined.

Nuclear import has been characterized through different ensemble methods, such as ensemble kinetic experiments [99] and FRAP [102]: knowledge of global reaction rates is however insufficient if one wishes to decipher the different steps underlying the tightly regulated transport process. Therefore, single-molecule tracking has become a powerful method in the field: by reducing the concentration of the observed fluorescent species, it is possible to spatially resolve single molecules and follow them as they undergo nuclear transport [103,104]. This technique has been successfully applied in order to measure the interaction times of several NTRs (e.g., Imp β, Imp α in [103]) as well as signal-dependent cargoes of different sizes (from BSA-NLS [103] to mRNA [105]).

Subviral nucleoprotein complexes or complete virus capsids exceed the size of such simple model substrates. A few examples of larger model cargoes have been characterized, e.g., quantum dots (QD, 30 nm) functionalized with multiple importin-binding domains [106]. These studies showed a high rejection rate at the cytoplasmic side of the NPC, and indicated that binding to multiple NTRs is necessary for efficient translocation of the large cargoes. Similarly, quantitative analysis of adenoviral nuclear import efficiency using bio-orthogonally labeled viral genomes showed that only a fraction of the incoming vDNA molecules entered the nucleus [80], but the mechanistic reason underlying this bottleneck is currently not understood.

The development of nanoscopic methods further provides us with the tools to image single NPCs with very high resolution in living cells. Stochastic super-resolution imaging visualized the eightfold symmetry of the nuclear pore and revealed the positioning of specific subcomplexes within the NPC [107,108], while fluorophore counting through iterative steps of photoconversion and bleaching yielded quantitative data allowing the estimation of subcomplex stoichiometry [109,110]. These novel methods offer the opportunity to detect specific NPC components which might play a role in viral entry into the nucleus or monitor potential rearrangements in NPC architecture induced by infection.

A system for directly studying molecular interactions of HIV-1 with the NPC has not yet been established. As a lentivirus, HIV-1 can infect nondividing cells and therefore must have developed strategies to translocate its genome across the nuclear envelope. However, composition and architecture of the subviral structure imported into the nucleus, as well as the nature of its karyophilic signal(s) remain to be determined [91,92]. Several individual HIV-1 proteins (Vpr, MA, IN) as well as the viral cDNA itself, have been proposed to serve as the relevant NLS [90,111]. In contrast, a crucial role of the viral capsid has emerged from more recent studies. Mutations that interfere with capsid stability affect postentry steps of the replication cycle [112]. Moreover, CA has been shown to interact with various cellular factors that affect nuclear import efficiency, including several nucleoporins [90,92,111]. Interestingly, the high-affinity binding site of at least two of these host factors (CPSF6 and Nup153), as well as of small molecule inhibitors as PF-74 that act on postentry stages, comprises residues from two adjacent CA monomers [113,114], suggesting that these molecules recognize the assembled capsid (or a capsid-like structure) retained throughout the transport to the nuclear pore. This is in agreement with strong CA signals detected on most cytoplasmic HIV-1 RTC/PIC by immunostaining [94] (Fig. 3 iv). Interestingly, while CA appeared to be absent on PICs observed in the nucleus of HeLa cells, it could be detected on nuclear PIC in primary macrophages, suggesting that CA remains associated with HIV-1 cDNA upon transport through the nuclear pore at least in some host cell types [94]. Albeit the use of immunostaining employed for CA detection in this study [94] due to the lack of a suitable direct label precluded quantitation of CA in the detected complexes, it is tempting to speculate that nuclear import of HIV-1 capsid-like structures may be possible in some cell types. With a diameter of ~ 50–60 nm at the broad end [115], the conical HIV-1 capsid exceeds the maximum diameter of the nuclear pore opening (~ 40 nm). If intact capsids or capsid-like structures were imported into the nucleus, structural and dynamic characterization of the process would not only yield important information on viral biology but also provide novel insights into nuclear pore function in human cells.

Virion structure and morphogenesis

In the late stages of the replication cycle, newly synthesized viral genomes and proteins assemble into progeny virions that subsequently exit from the host cell. Many enveloped viruses such as HIV-1 assemble at the plasma membrane of the host cell where virus buds are released by abscission of the viral envelope.

HIV-1 particle formation is orchestrated by the Gag polyprotein. Gag self-assembles at the cytoplasmic site of the plasma membrane and mediates the recruitment of other viral proteins (Env, Vpr, and the viral enzymes incorporated as GagPol polyprotein), the vRNA genome, and host cell factors required for release to the nascent bud [116]. Concomitant with particle release, Gag is processed by the virus-encoded protease (PR), resulting in the rearrangement of the incomplete spherical Gag shell into the conical capsid encasing vRNA and replication proteins. This proteolytic maturation is essential for HIV-1 infectivity [117]. Although the structure of the immature HIV-1 Gag layer and the mature capsid have been analyzed in detail by electron microscopy (EM)-based methods [118], these studies provided only static images of the regular protein lattices. In contrast, the structure of maturation intermediates and the dynamics of the complex rearrangements in virus architecture, as well as the precise localization of other important components (GagPol, Env, vRNA) at budding sites and in particles, are poorly characterized.

Nanoscopic methods now provide the possibility to visualize subviral structures at the assembly site and within the virion. In recent years, novel insights into the arrangement of Gag, Env, and host cell proteins at HIV-1 assembly sites have been gained by nanoscopy. However, these studies almost exclusively relied on the use of FP derivatives and immunostaining. Photoactivatable or photoswitchable FPs were inserted either at the C-terminus of Gag expressed by itself [15,41,42,119–121], or between the MA and CA domains of Gag in the viral context [43]. While Gag-FP-tagged particles are efficiently released, expression of FP-tagged variants alone results in accumulation of Gag-FP patches at the plasma membrane [25] and release of virus-like particles with a discontinuous Gag layer [122], indicating that the presence of the FP-tag affects Gag lattice formation. Quantitative PALM cluster analysis revealed a notable influence of the type of FP-tag used on the size and density of Gag-FP assembly sites detected [41]. Image analyses of HIV-1 assembly sites [8] therefore mainly employ complementation with untagged Gag or virus, which rescues morphology and infectivity of FP-tagged derivatives [25].

Insertion of a SNAP-tag into HIV-1 Gag yields a virus that still requires wild-type complementation, but displays higher replication capacity than the corresponding FP-tagged variants and permits staining of Gag with bright synthetic fluorophores in live cells [123]. The application of this derivative provided high-

resolution dSTORM images of virus buds with a size comparable to that derived from electron tomography and a Gag distribution corresponding to the 2D projection of a truncated sphere [124] (Fig. 3 v). HIV-1 carrying a TC-tag in the same position exhibits near wild-type replication capacity [125] and was used to monitor transmission of viral structural protein from infected macrophages [125] (Fig. 3 ix) or immature dendritic cells [126] through virological synapses by live cell imaging. Comparison with immunostaining revealed a redox-dependent bias of TC-tag detection for intracellular immature Gag over released particles under imaging conditions in the latter study [126], and the variant has not yet been employed for single molecule-based applications.

In contrast, HIV-1 carrying a TC-tag to the C-terminus of IN was used to discriminate between immature and mature particles and to characterize the size of subviral complexes detected in the cytoplasm or nucleus by PALM [127] (Fig. 3 viii). Distinction between different morphologies required extensive image analysis, however, and the time resolution achieved in live cells was low. Detection of HIV-1 Env or cellular proteins at HIV-1 assembly sites for SRFM analyses [8] was so far performed almost exclusively by immuno-staining, which impairs effective localization precision and precludes live cell imaging for intracellular POI. Development of structural proteins carrying minimally invasive synthetic labels appears crucial to fully exploit the potential of nanoscopic techniques for studying the architecture of viral budding sites and particles.

Labeling of the influenza virus HA glycoprotein on the surface of virus producing cells has been accomplished using either a Sortase-tag [128] (Fig. 3vii) or amber suppression/click chemistry [77] (Fig. 3vi); these derivatives should allow the analysis of influenza virus formation by advanced fluorescence methods. Likewise, the recently described A1/Q3 tagging of HIV-1 Env [88] offers new possibilities for studying HIV-1 morphogenesis and Env dynamics under live cell conditions. Exploitation of minimally invasive labeling strategies together with advancements in microscopic resolution can be expected to yield more detailed insights in the recruitment of proteins and lipids to HIV-1 assembly sites and in the maturation process in the near future.

Current challenges

Despite many advantages, current chemical labeling strategies have limitations with respect to their use in live eukaryotic cells. This particularly refers to properties of synthetic fluorophores and the application of amber suppression technology for virus production.

Many available synthetic fluorophores, including particularly bright and photostable ones, are noncell-permeable and can thus only target molecules displayed at the cell or particle surface (e.g., viral envelope glycoproteins or receptors on the host cell surface). For cell-permeable dyes, cell uptake and coupling to or association with the target may represent non-negligible rate-limiting steps.

Furthermore, while genetic linkage of the fluorophore to the POI leads to exclusive molecular labeling specificity in the case of FP, residual unspecific labeling can become a relevant concern in the case of synthetic dyes equipped only with limited biorthogonal chemical reactivities. Nonspecific sticking and aggregation of hydrophobic dyes may result in high background and reduce the contrast to a level incompatible with nanoscopic techniques.

An advancement is brought about by cell-permeable, relatively nontoxic, fluorogenic dyes, which allow more specific detection of the protein of interest in live cells or tissues without the need for washing steps [129,130]. This principle is exemplified by the recently described near-infrared dye silicone rhodamine (SiR), shown to be applicable for nanoscopy as well as for live cell imaging in tissues, and available in the form of various functionalized derivatives [131,132]. SiR and similar fluorogenic dye concepts (e.g., [133]) should greatly expand experimental options for virological studies.

Targeted insertion of ncAA followed by click labeling is a very elegant protein labeling strategy, but its practical application in virology is not trivial. To date, the approach is best established for *E. coli*, which is characterized by very infrequent use of TAG as a stop codon (~ 7% of all ORFs), while this codon is more frequently found in eukaryotic cells required for studying pathogenic viruses (~ 20% of ORFs terminate with TAG). Furthermore, virus-encoded genes also employ amber stop codons (e.g., 5 of 9 ORF in the HIV-1_{NL4-3} genome end with TAG) whose untargeted read-through may result in unwanted side effects when applying amber suppression for viral protein labeling. Most importantly, limited suppression efficiency still hampers application of the strategy in human cells and may result in protein levels insufficient to sustain virus production. Type, fidelity, and expression levels of the tRNA/RS pair have a strong influence on the expression yield, which indicates directions for further optimization [66]. Moreover, strategies to alter release factor specificity or engineering of quadruplet codons may emerge as efficient tools to address many of the current limitations [134–137].

Concluding remarks

Novel labeling and imaging techniques expand the toolbox of virologists and provide them with new opportunities for quantitative studies of individual steps in virus replication. While the application of these techniques still presents experimental challenges, the field is starting to progress beyond proof-of-principle studies toward addressing new virological questions. Supported by very active research on minimally invasive labeling strategies and synthetic dyes, quantitative insights into viral replication that were previously challenging to approach are now within grasp.

Acknowledgements

Work in the laboratories of the authors is in part funded by the Deutsche Forschungsgemeinschaft through the Sonderforschungsbereich 1129, project 6 (BM), and project 7 (EAL).

Author Contribution

VS, GP, EAL and BM wrote the manuscript, VS and BM prepared figures.

References

1 Giepmans BN, Adams SR, Ellisman MH and Tsien RY (2006) The fluorescent toolbox for assessing protein location and function. *Science* **312**, 217–224.
2 Nienhaus K and Nienhaus GU (2014) Fluorescent proteins for live-cell imaging with super-resolution. *Chem Soc Rev* **43**, 1088–1106.
3 Machan R and Wohland T (2014) Recent applications of fluorescence correlation spectroscopy in live systems. *FEBS Lett* **588**, 3571–3584.
4 Wiseman PW (2015) Image correlation spectroscopy: principles and applications. *Cold Spring Harb Protoc* **2015**, 336–348.
5 Milles S and Lemke EA (2013) What precision-protein-tuning and nano-resolved single molecule sciences can do for each other. *BioEssays* **35**, 65–74.
6 Hell SW (2007) Far-field optical nanoscopy. *Science* **316**, 1153–1158.
7 Huang B, Bates M and Zhuang X (2009) Super-resolution fluorescence microscopy. *Annu Rev Biochem* **78**, 993–1016.
8 Hanne J, Zila V, Heilemann M, Müller B, Kräusslich HG (2016) Super-resolved insights into human immunodeficiency virus biology. *FEBS Lett*, doi: 10.1002/1873-3468.
9 Baumgartel V, Muller B and Lamb DC (2012) Quantitative live-cell imaging of human immunodeficiency virus (HIV-1) assembly. *Viruses* **4**, 777–799.
10 Boulant S, Stanifer M and Lozach PY (2015) Dynamics of virus-receptor interactions in virus binding, signaling, and endocytosis. *Viruses* **7**, 2794–2815.
11 Brandenburg B and Zhuang X (2007) Virus trafficking – learning from single-virus tracking. *Nat Rev Microbiol* **5**, 197–208.
12 Rust MJ, Lakadamyali M, Brandenburg B and Zhuang X (2011) Single-virus tracking in live cells. *Cold Spring Harb Protoc*, doi: 10.1101/pdb.top065623.
13 Fackler OT, Murooka TT, Imle A and Mempel TR (2014) Adding new dimensions: towards an integrative understanding of HIV-1 spread. *Nat Rev Microbiol* **12**, 563–574.
14 Hell SW and Wichmann J (1994) Breaking the diffraction resolution limit by stimulated emission: stimulated-emission-depletion fluorescence microscopy. *Opt Lett* **19**, 780–782.
15 Betzig E, Patterson GH, Sougrat R, Lindwasser OW, Olenych S, Bonifacino JS, Davidson MW, Lippincott-Schwartz J and Hess HF (2006) Imaging intracellular fluorescent proteins at nanometer resolution. *Science* **313**, 1642–1645.
16 Hess ST, Girirajan TP and Mason MD (2006) Ultra-high resolution imaging by fluorescence photoactivation localization microscopy. *Biophys J* **91**, 4258–4272.
17 Rust MJ, Bates M and Zhuang X (2006) Sub-diffraction-limit imaging by stochastic optical reconstruction microscopy (STORM). *Nat Methods* **3**, 793–795.
18 Campbell EM and Hope TJ (2008) Live cell imaging of the HIV-1 life cycle. *Trends Microbiol* **16**, 580–587.
19 Chojnacki J and Muller B (2013) Investigation of HIV-1 assembly and release using modern fluorescence imaging techniques. *Traffic* **14**, 15–24.
20 McDonald D, Vodicka MA, Lucero G, Svitkina TM, Borisy GG, Emerman M and Hope TJ (2002) Visualization of the intracellular behavior of HIV in living cells. *J Cell Biol* **159**, 441–452.
21 Albanese A, Arosio D, Terreni M and Cereseto A (2008) HIV-1 pre-integration complexes selectively target decondensed chromatin in the nuclear periphery. *PLoS One* **3**, e2413.
22 Hermida-Matsumoto L and Resh MD (2000) Localization of human immunodeficiency virus type 1 Gag and Env at the plasma membrane by confocal imaging. *J Virol* **74**, 8670–8679.
23 Perrin-Tricaud C, Davoust J and Jones IM (1999) Tagging the human immunodeficiency virus gag protein with green fluorescent protein. Minimal evidence for colocalisation with actin. *Virology* **255**, 20–25.
24 Hubner W, Chen P, Del Portillo A, Liu Y, Gordon RE and Chen BK (2007) Sequence of human

immunodeficiency virus type 1 (HIV-1) Gag localization and oligomerization monitored with live confocal imaging of a replication-competent, fluorescently tagged HIV-1. *J Virol* **81**, 12596–12607.
25 Muller B, Daecke J, Fackler OT, Dittmar MT, Zentgraf H and Krausslich HG (2004) Construction and characterization of a fluorescently labeled infectious human immunodeficiency virus type 1 derivative. *J Virol* **78**, 10803–10813.
26 Hendrix J, Baumgärtel V, Schrimpf W, Ivanchenko S, Digman MA, Gratton E, Kräusslich HG, Müller B and Lamb DC (2015) Live-cell observation of cytosolic HIV-1 assembly onset reveals RNA-interacting Gag oligomers. *J Cell Biol* **210**, 629–646.
27 El Meshri SE, Dujardin D, Godet J, Richert L, Boudier C, Darlix JL, Didier P, Mely Y and de Rocquigny H (2015) Role of the nucleocapsid domain in HIV-1 Gag oligomerization and trafficking to the plasma membrane: a fluorescence lifetime imaging microscopy investigation. *J Mol Biol* **427**, 1480–1494.
28 Jouvenet N, Bieniasz PD and Simon SM (2008) Imaging the biogenesis of individual HIV-1 virions in live cells. *Nature* **454**, 236–240.
29 Ivanchenko S, Godinez WJ, Lampe M, Kräusslich HG, Eils R, Rohr K, Brauchle C, Müller B and Lamb DC (2009) Dynamics of HIV-1 assembly and release. *PLoS Pathog* **5**, e1000652.
30 Baumgärtel V, Ivanchenko S, Dupont A, Sergeev M, Wiseman PW, Kräusslich HG, Brauchle C, Müller B, Lamb DC *et al.* (2011) Live-cell visualization of dynamics of HIV budding site interactions with an ESCRT component. *Nat Cell Biol* **13**, 469–474.
31 Jouvenet N, Simon SM and Bieniasz PD (2009) Imaging the interaction of HIV-1 genomes and Gag during assembly of individual viral particles. *Proc Natl Acad Sci USA* **106**, 19114–19119.
32 Jouvenet N, Zhadina M, Bieniasz PD and Simon SM (2011) Dynamics of ESCRT protein recruitment during retroviral assembly. *Nat Cell Biol* **13**, 394–401.
33 Miyauchi K, Marin M and Melikyan GB (2011) Visualization of retrovirus uptake and delivery into acidic endosomes. *Biochem J* **434**, 559–569.
34 Herold N, Anders-Osswein M, Glass B, Eckhardt M, Muller B and Krausslich HG (2014) HIV-1 entry in SupT1-R5, CEM-ss, and primary CD4+ T cells occurs at the plasma membrane and does not require endocytosis. *J Virol* **88**, 13956–13970.
35 Izquierdo-Useros N, Lorizate M, Puertas MC, Rodriguez-Plata MT, Zangger N, Erikson E, Pino M, Erkizia I, Glass B, Clotet B *et al.* (2012) Siglec-1 is a novel dendritic cell receptor that mediates HIV-1 trans-infection through recognition of viral membrane gangliosides. *PLoS Biol* **10**, e1001448.
36 Chen J, Nikolaitchik O, Singh J, Wright A, Bencsics CE, Coffin JM, Ni N, Lockett S, Pathak VK and Hu WS (2009) High efficiency of HIV-1 genomic RNA packaging and heterozygote formation revealed by single virion analysis. *Proc Natl Acad Sci USA* **106**, 13535–13540.
37 Chen J, Rahman SA, Nikolaitchik OA, Grunwald D, Sardo L, Burdick RC, Plisov S, Liang E, Tai S, Pathak VK *et al.* (2016) HIV-1 RNA genome dimerizes on the plasma membrane in the presence of Gag protein. *Proc Natl Acad Sci USA* **113**, E201–E208.
38 Itano MS, Bleck M, Johnson DS and Simon SM (2016) Readily accessible multiplane microscopy: 3D tracking the HIV-1 genome in living cells. *Traffic* **17**, 179–186.
39 Miyauchi K, Kim Y, Latinovic O, Morozov V and Melikyan GB (2009) HIV enters cells via endocytosis and dynamin-dependent fusion with endosomes. *Cell* **137**, 433–444.
40 Mamede JI and Hope TJ (2016) Detection and tracking of dual-labeled HIV particles using wide-field live cell imaging to follow viral core integrity. *Methods Mol Biol* **1354**, 49–59.
41 Gunzenhauser J, Olivier N, Pengo T and Manley S (2012) Quantitative super-resolution imaging reveals protein stoichiometry and nanoscale morphology of assembling HIV-Gag virions. *Nano Lett* **12**, 4705–4710.
42 Lehmann M, Rocha S, Mangeat B, Blanchet F, Uji IH, Hofkens J and Piguet V (2011) Quantitative multicolor super-resolution microscopy reveals tetherin HIV-1 interaction. *PLoS Pathog* **7**, e1002456.
43 Muranyi W, Malkusch S, Muller B, Heilemann M and Krausslich HG (2013) Super-resolution microscopy reveals specific recruitment of HIV-1 envelope proteins to viral assembly sites dependent on the envelope C-terminal tail. *PLoS Pathog* **9**, e1003198.
44 Lehmann MJ, Sherer NM, Marks CB, Pypaert M and Mothes W (2005) Actin- and myosin-driven movement of viruses along filopodia precedes their entry into cells. *J Cell Biol* **170**, 317–325.
45 Murooka TT, Deruaz M, Marangoni F, Vrbanac VD, Seung E, von Andrian UH, Tager AM, Luster AD and Mempel TR (2012) HIV-infected T cells are migratory vehicles for viral dissemination. *Nature* **490**, 283–287.
46 Sewald X, Gonzalez DG, Haberman AM and Mothes W (2012) In vivo imaging of virological synapses. *Nat Commun* **3**, 1320.
47 Sewald X, Ladinsky MS, Uchil PD, Beloor J, Pi R, Herrmann C, Motamedi N, Murooka TT, Brehm MA, Greiner DL *et al.* (2015) Retroviruses use CD169-mediated trans-infection of permissive lymphocytes to establish infection. *Science* **350**, 563–567.

48 Mishin AS, Belousov VV, Solntsev KM and Lukyanov KA (2015) Novel uses of fluorescent proteins. *Curr Opin Chem Biol* **27**, 1–9.
49 Craggs TD (2009) Green fluorescent protein: structure, folding and chromophore maturation. *Chem Soc Rev* **38**, 2865–2875.
50 Costantini LM and Snapp EL (2015) Going viral with fluorescent proteins. *J Virol* **89**, 9706–9708.
51 Costantini LM, Fossati M, Francolini M and Snapp EL (2012) Assessing the tendency of fluorescent proteins to oligomerize under physiologic conditions. *Traffic* **13**, 643–649.
52 Keppler A, Gendreizig S, Gronemeyer T, Pick H, Vogel H and Johnsson K (2003) A general method for the covalent labeling of fusion proteins with small molecules in vivo. *Nat Biotechnol* **21**, 86–89.
53 Gautier A, Juillerat A, Heinis C, Correa IR Jr, Kindermann M, Beaufils F and Johnsson K (2008) An engineered protein tag for multiprotein labeling in living cells. *Chem Biol* **15**, 128–136.
54 Los GV, Encell LP, McDougall MG, Hartzell DD, Karassina N, Zimprich C, Wood MG, Learish R, Ohana RF, Urh M *et al.* (2008) HaloTag: a novel protein labeling technology for cell imaging and protein analysis. *ACS Chem Biol* **3**, 373–382.
55 Wombacher R, Heidbreder M, van de Linde S, Sheetz MP, Heilemann M, Cornish VW and Sauer M (2010) Live-cell super-resolution imaging with trimethoprim conjugates. *Nat Methods* **7**, 717–719.
56 Adams SR, Campbell RE, Gross LA, Martin BR, Walkup GK, Yao Y, Llopis J and Tsien RY (2002) New biarsenical ligands and tetracysteine motifs for protein labeling in vitro and in vivo: synthesis and biological applications. *J Am Chem Soc* **124**, 6063–6076.
57 Popp MW, Antos JM, Grotenbreg GM, Spooner E and Ploegh HL (2007) Sortagging: a versatile method for protein labeling. *Nat Chem Biol* **3**, 707–708.
58 Lin CW and Ting AY (2006) Transglutaminase-catalyzed site-specific conjugation of small-molecule probes to proteins in vitro and on the surface of living cells. *J Am Chem Soc* **128**, 4542–4543.
59 Yin J, Straight PD, McLoughlin SM, Zhou Z, Lin AJ, Golan DE, Kelleher NL, Kolter R and Walsh CT (2005) Genetically encoded short peptide tag for versatile protein labeling by Sfp phosphopantetheinyl transferase. *Proc Natl Acad Sci USA* **102**, 15815–15820.
60 Zhou Z, Koglin A, Wang Y, McMahon AP and Walsh CT (2008) An eight residue fragment of an acyl carrier protein suffices for post-translational introduction of fluorescent pantetheinyl arms in protein modification in vitro and in vivo. *J Am Chem Soc* **130**, 9925–9930.
61 Fernandez-Suarez M, Baruah H, Martinez-Hernandez L, Xie KT, Baskin JM, Bertozzi CR and Ting AY (2007) Redirecting lipoic acid ligase for cell surface protein labeling with small-molecule probes. *Nat Biotechnol* **25**, 1483–1487.
62 Uttamapinant C, White KA, Baruah H, Thompson S, Fernández-Suárez M, Puthenveetil S and Ting AY (2010) A fluorophore ligase for site-specific protein labeling inside living cells. *Proc Natl Acad Sci U S A* **107**, 10914–10919.
63 Cohen GN and Munier R (1956) Incorporation of structural analogues of amino acids in bacterial proteins. *Biochim Biophys Acta* **21**, 592–593.
64 Ngo JT and Tirrell DA (2011) Noncanonical amino acids in the interrogation of cellular protein synthesis. *Acc Chem Res* **44**, 677–685.
65 Liu DR and Schultz PG (1999) Progress toward the evolution of an organism with an expanded genetic code. *Proc Natl Acad Sci USA* **96**, 4780–4785.
66 Liu CC and Schultz PG (2010) Adding new chemistries to the genetic code. *Annu Rev Biochem* **79**, 413–444.
67 Elliott TS, Townsley FM, Bianco A, Ernst RJ, Sachdeva A, Elsasser SJ, Davis L, Lang K, Pisa R, Greiss S *et al.* (2014) Proteome labeling and protein identification in specific tissues and at specific developmental stages in an animal. *Nat Biotechnol* **32**, 465–472.
68 Greiss S and Chin JW (2011) Expanding the genetic code of an animal. *J Am Chem Soc* **133**, 14196–14199.
69 Lemke EA (2014) The exploding genetic code. *ChemBioChem* **15**, 1691–1694.
70 Nikic I and Lemke EA (2015) Genetic code expansion enabled site-specific dual-color protein labeling: superresolution microscopy and beyond. *Curr Opin Chem Biol* **28**, 164–173.
71 Hackenberger CP and Schwarzer D (2008) Chemoselective ligation and modification strategies for peptides and proteins. *Angew Chem Int Ed Engl* **47**, 10030–10074.
72 van Hest JC and van Delft FL (2011) Protein modification by strain-promoted alkyne-azide cycloaddition. *ChemBioChem* **12**, 1309–1312.
73 Sauer J, Mielert A, Lang D and Peter D (1965) Eine Studie der Diels-Alder-Reaktion, III: Umsetzungen von 1.2.4.5-Tetrazinen mit Olefinen. Zur Struktur von Dihydropyridazinen. *Chem Ber* **98**, 1435–1445.
74 Wiessler M, Waldeck W, Kliem C, Pipkorn R and Braun K (2009) The Diels-Alder-reaction with inverse-electron-demand, a very efficient versatile click-reaction concept for proper ligation of variable molecular partners. *Int J Med Sci* **7**, 19–28.
75 Devaraj NK, Weissleder R and Hilderbrand SA (2008) Tetrazine-based cycloadditions: application to pretargeted live cell imaging. *Bioconjug Chem* **19**, 2297–2299.

76 Lin S, Yan H, Li L, Yang M, Peng B, Chen S, Li W and Chen PR (2013) Site-specific engineering of chemical functionalities on the surface of live hepatitis D virus. *Angew Chem Int Ed Engl* **52**, 13970–13974.

77 Nikic I, Plass T, Schraidt O, Szymanski J, Briggs JA, Schultz C and Lemke EA (2014) Minimal tags for rapid dual-color live-cell labeling and super-resolution microscopy. *Angew Chem Int Ed Engl* **53**, 2245–2249.

78 Jao CY and Salic A (2008) Exploring RNA transcription and turnover in vivo by using click chemistry. *Proc Natl Acad Sci USA* **105**, 15779–15784.

79 Salic A and Mitchison TJ (2008) A chemical method for fast and sensitive detection of DNA synthesis in vivo. *Proc Natl Acad Sci USA* **105**, 2415–2420.

80 Wang IH, Suomalainen M, Andriasyan V, Kilcher S, Mercer J, Neef A, Luedtke NW and Greber UF (2013) Tracking viral genomes in host cells at single-molecule resolution. *Cell Host Microbe* **14**, 468–480.

81 Xu H, Franks T, Gibson G, Huber K, Rahm N, Strambio De Castillia C, Luban J, Aiken C, Watkins S, Sluis-Cremer N *et al.* (2013) Evidence for biphasic uncoating during HIV-1 infection from a novel imaging assay. *Retrovirology* **10**, 70.

82 Jewett JC and Bertozzi CR (2010) Cu-free click cycloaddition reactions in chemical biology. *Chem Soc Rev* **39**, 1272–1279.

83 Rubino FA, Oum YH, Rajaram L, Chu Y and Carrico IS (2012) Chemoselective modification of viral surfaces via bioorthogonal click chemistry. *J Vis Exp* **19**, e4246.

84 Kuerschner L and Thiele C (2014) Multiple bonds for the lipid interest. *Biochim Biophys Acta* **1841**, 1031–1037.

85 Checkley MA, Luttge BG and Freed EO (2011) HIV-1 envelope glycoprotein biosynthesis, trafficking, and incorporation. *J Mol Biol* **410**, 582–608.

86 Pereira CF, Ellenberg PC, Jones KL, Fernandez TL, Smyth RP, Hawkes DJ, Hijnen M, Vivet-Boudou V, Marquet R, Johnson I *et al.* (2011) Labeling of multiple HIV-1 proteins with the biarsenical-tetracysteine system. *PLoS One* **6**, e17016.

87 Nakane S, Iwamoto A and Matsuda Z (2015) The V4 and V5 variable loops of HIV-1 envelope glycoprotein are tolerant to insertion of green fluorescent protein and are useful targets for labeling. *J Biol Chem* **290**, 15279–15291.

88 Munro JB, Gorman J, Ma X, Zhou Z, Arthos J, Burton DR, Koff WC, Courter JR, Smith AB, 3rd, Kwong PD *et al.* (2014) Conformational dynamics of single HIV-1 envelope trimers on the surface of native virions. *Science* **346**, 759–763.

89 Ruthardt N, Lamb DC and Brauchle C (2011) Single-particle tracking as a quantitative microscopy-based approach to unravel cell entry mechanisms of viruses and pharmaceutical nanoparticles. *Mol Ther* **19**, 1199–1211.

90 Matreyek KA and Engelman A (2013) Viral and cellular requirements for the nuclear entry of retroviral preintegration nucleoprotein complexes. *Viruses* **5**, 2483–2511.

91 Ambrose Z and Aiken C (2014) HIV-1 uncoating: connection to nuclear entry and regulation by host proteins. *Virology* **454–455**, 371–379.

92 Campbell EM and Hope TJ (2015) HIV-1 capsid: the multifaceted key player in HIV-1 infection. *Nat Rev Microbiol* **13**, 471–483.

93 Arhel N, Genovesio A, Kim KA, Miko S, Perret E, Olivo-Marin JC, Shorte S and Charneau P (2006) Quantitative four-dimensional tracking of cytoplasmic and nuclear HIV-1 complexes. *Nat Methods* **3**, 817–824.

94 Peng K, Muranyi W, Glass B, Laketa V, Yant SR, Tsai L, Cihlar T, Müller B and Kräusslich HG (2014) Quantitative microscopy of functional HIV post-entry complexes reveals association of replication with the viral capsid. *Elife* **3**, e04114.

95 Campbell EM, Perez O, Anderson JL and Hope TJ (2008) Visualization of a proteasome-independent intermediate during restriction of HIV-1 by rhesus TRIM5alpha. *J Cell Biol* **180**, 549–561.

96 Rihn SJ, Wilson SJ, Loman NJ, Alim M, Bakker SE, Bhella D, Gifford RJ, Rixon FJ and Bieniasz PD (2013) Extreme genetic fragility of the HIV-1 capsid. *PLoS Pathog* **9**, e1003461.

97 von Schwedler UK, Stray KM, Garrus JE and Sundquist WI (2003) Functional surfaces of the human immunodeficiency virus type 1 capsid protein. *J Virol* **77**, 5439–5450.

98 von Appen A, Kosinski J, Sparks L, Ori A, DiGuilio AL, Vollmer B, Mackmull MT, Banterle N, Parca L, Kastritis P *et al.* (2015) In situ structural analysis of the human nuclear pore complex. *Nature* **526**, 140–143.

99 Ribbeck K and Gorlich D (2001) Kinetic analysis of translocation through nuclear pore complexes. *EMBO J* **20**, 1320–1330.

100 Mettenleiter TC (2015) Breaching the barrier-the nuclear envelope in virus infection. *J Mol Biol*, doi: 10.1016/j.jmb.2015.10.001.

101 Labokha AA and Fassati A (2013) Viruses challenge selectivity barrier of nuclear pores. *Viruses* **5**, 2410–2423.

102 Naim B, Brumfeld V, Kapon R, Kiss V, Nevo R and Reich Z (2007) Passive and facilitated transport in nuclear pore complexes is largely uncoupled. *J Biol Chem* **282**, 3881–3888.

103 Dange T, Grunwald D, Grunwald A, Peters R and Kubitscheck U (2008) Autonomy and robustness of translocation through the nuclear pore complex: a single-molecule study. *J Cell Biol* **183**, 77–86.

104 Yang W, Gelles J and Musser SM (2004) Imaging of single-molecule translocation through nuclear pore complexes. *Proc Natl Acad Sci USA* **101**, 12887–12892.

105 Grunwald D and Singer RH (2010) In vivo imaging of labelled endogenous beta-actin mRNA during nucleocytoplasmic transport. *Nature* **467**, 604–607.
106 Lowe AR, Siegel JJ, Kalab P, Siu M, Weis K and Liphardt JT (2010) Selectivity mechanism of the nuclear pore complex characterized by single cargo tracking. *Nature* **467**, 600–603.
107 Loschberger A, van de Linde S, Dabauvalle MC, Rieger B, Heilemann M, Krohne G and Sauer M (2012) Super-resolution imaging visualizes the eightfold symmetry of gp210 proteins around the nuclear pore complex and resolves the central channel with nanometer resolution. *J Cell Sci* **125**, 570–575.
108 Szymborska A, de Marco A, Daigle N, Cordes VC, Briggs JA and Ellenberg J (2013) Nuclear pore scaffold structure analyzed by super-resolution microscopy and particle averaging. *Science* **341**, 655–658.
109 Ori A, Banterle N, Iskar M, Andres-Pons A, Escher C, Khanh Bui H, Sparks L, Solis-Mezarino V, Rinner O, Bork P *et al.* (2013) Cell type-specific nuclear pores: a case in point for context-dependent stoichiometry of molecular machines. *Mol Syst Biol* **9**, 648.
110 Banterle N, Bui KH, Lemke EA and Beck M (2013) Fourier ring correlation as a resolution criterion for super-resolution microscopy. *J Struct Biol* **183**, 363–367.
111 Hilditch L and Towers GJ (2014) A model for cofactor use during HIV-1 reverse transcription and nuclear entry. *Curr Opin Virol* **4**, 32–36.
112 Forshey BM, von Schwedler U, Sundquist WI and Aiken C (2002) Formation of a human immunodeficiency virus type 1 core of optimal stability is crucial for viral replication. *J Virol* **76**, 5667–5677.
113 Bhattacharya A, Alam SL, Fricke T, Zadrozny K, Sedzicki J, Taylor AB, Demeler B, Pornillos O, Ganser-Pornillos BK, Diaz-Griffero F *et al.* (2014) Structural basis of HIV-1 capsid recognition by PF74 and CPSF6. *Proc Natl Acad Sci USA* **111**, 18625–18630.
114 Price AJ, Jacques DA, McEwan WA, Fletcher AJ, Essig S, Chin JW, Halambage UD, Aiken C and James LC (2014) Host cofactors and pharmacologic ligands share an essential interface in HIV-1 capsid that is lost upon disassembly. *PLoS Pathog* **10**, e1004459.
115 Briggs JA, Wilk T, Welker R, Krausslich HG and Fuller SD (2003) Structural organization of authentic, mature HIV-1 virions and cores. *EMBO J* **22**, 1707–1715.
116 Sundquist WI and Krausslich HG (2012) HIV-1 assembly, budding, and maturation. *Cold Spring Harb Perspect Med* **2**, a006924.
117 Konvalinka J, Kräusslich HG and Müller B (2015) Retroviral proteases and their roles in virion maturation. *Virology* **479–480**, 403–417.
118 Briggs JA and Krausslich HG (2011) The molecular architecture of HIV. *J Mol Biol* **410**, 491–500.
119 Manley S, Gillette JM, Patterson GH, Shroff H, Hess HF, Betzig E and Lippincott-Schwartz J (2008) High-density mapping of single-molecule trajectories with photoactivated localization microscopy. *Nat Methods* **5**, 155–157.
120 Van Engelenburg SB, Shtengel G, Sengupta P, Waki K, Jarnik M, Ablan SD, Freed EO, Hess HF and Lippincott-Schwartz J (2014) Distribution of ESCRT machinery at HIV assembly sites reveals virus scaffolding of ESCRT subunits. *Science* **343**, 653–656.
121 Bleck M, Itano MS, Johnson DS, Thomas VK, North AJ, Bieniasz PD and Simon SM (2014) Temporal and spatial organization of ESCRT protein recruitment during HIV-1 budding. *Proc Natl Acad Sci USA* **111**, 12211–12216.
122 Pornillos O, Higginson DS, Stray KM, Fisher RD, Garrus JE, Payne M, He GP, Wang HE, Morham SG and Sundquist WI (2003) HIV Gag mimics the Tsg101-recruiting activity of the human Hrs protein. *J Cell Biol* **162**, 425–434.
123 Eckhardt M, Anders M, Muranyi W, Heilemann M, Krijnse-Locker J and Muller B (2011) A SNAP-tagged derivative of HIV-1–a versatile tool to study virus-cell interactions. *PLoS One* **6**, e22007.
124 Malkusch S, Muranyi W, Muller B, Krausslich HG and Heilemann M (2013) Single-molecule coordinate-based analysis of the morphology of HIV-1 assembly sites with near-molecular spatial resolution. *Histochem Cell Biol* **139**, 173–179.
125 Gousset K, Ablan SD, Coren LV, Ono A, Soheilian F, Nagashima K, Ott DE and Freed EO (2008) Real-time visualization of HIV-1 GAG trafficking in infected macrophages. *PLoS Pathog* **4**, e1000015.
126 Turville SG, Aravantinou M, Stossel H, Romani N and Robbiani M (2008) Resolution of de novo HIV production and trafficking in immature dendritic cells. *Nat Methods* **5**, 75–85.
127 Lelek M, Di Nunzio F, Henriques R, Charneau P, Arhel N and Zimmer C (2012) Superresolution imaging of HIV in infected cells with FlAsH-PALM. *Proc Natl Acad Sci USA* **109**, 8564–8569.
128 Popp MW, Karssemeijer RA and Ploegh HL (2012) Chemoenzymatic site-specific labeling of influenza glycoproteins as a tool to observe virus budding in real time. *PLoS Pathog* **8**, e1002604.
129 Jullien L and Gautier A (2015) Fluorogen-based reporters for fluorescence imaging: a review. *Methods Appl Fluoresc* **3**, e042007.
130 Bruchez MP (2015) Dark dyes-bright complexes: fluorogenic protein labeling. *Curr Opin Chem Biol* **27**, 18–23.
131 Lukinavicius G, Umezawa K, Olivier N, Honigmann A, Yang G, Plass T, Mueller V, Reymond L, Correa

IR Jr, Luo ZG *et al*. (2013) A near-infrared fluorophore for live-cell super-resolution microscopy of cellular proteins. *Nat Chem* **5**, 132–139.
132 Lukinavicius G, Blaukopf C, Pershagen E, Schena A, Reymond L, Derivery E, Gonzalez-Gaitan M, D'Este E, Hell SW, Gerlich DW *et al*. (2015) SiR-Hoechst is a far-red DNA stain for live-cell nanoscopy. *Nat Commun* **6**, 8497.
133 Herner A, Estrada Girona G, Nikic I, Kallay M, Lemke EA and Kele P (2014) New generation of bioorthogonally applicable fluorogenic dyes with visible excitations and large Stokes shifts. *Bioconjug Chem* **25**, 1370–1374.
134 Mukai T, Hayashi A, Iraha F, Sato A, Ohtake K, Yokoyama S and Sakamoto K (2010) Codon reassignment in the *Escherichia coli* genetic code. *Nucleic Acids Res* **38**, 8188–8195.
135 Johnson DB, Xu J, Shen Z, Takimoto JK, Schultz MD, Schmitz RJ, Xiang Z, Ecker JR, Briggs SP and Wang L (2011) RF1 knockout allows ribosomal incorporation of unnatural amino acids at multiple sites. *Nat Chem Biol* **7**, 779–786.
136 Neumann H, Wang KH, Davis L, Garcia-Alai M and Chin JW (2010) Encoding multiple unnatural amino acids via evolution of a quadruplet-decoding ribosome. *Nature* **464**, 441–444.
137 Schmied WH, Elsasser SJ, Uttamapinant C and Chin JW (2014) Efficient multisite unnatural amino acid incorporation in mammalian cells via optimized pyrrolysyl tRNA synthetase/tRNA expression and engineered eRF1. *J Am Chem Soc* **136**, 15577–15583.
138 Tcherkasskaya O, Davidson EA and Uversky VN (2003) Biophysical constraints for protein structure prediction. *J Proteome Res* **2**, 37–42.
139 Flatt JW and Greber UF (2015) Misdelivery at the nuclear pore complex-stopping a virus dead in its tracks. *Cells* **4**, 277–296.